International Journal of Engineering, Sciences and Technologies
ISSN : 3079-2045
https://www.ij-est.org/
Volume 2, issue 1, https://doi.org/10.70961/IKDY7329

Satellite observations of aerosol and precursor gas distribution in Madagascar

Mbolanjara H. ANDRIAMAMONJY[1], Anzelà M. RAMAROSANDRATANA[2], Richard RAMAROSON[3]

1- PhD student, Ecole Doctorale Ingénierie et Géosciences, 101 Antananarivo, Madagascar
2- PhD student, Sciences et Techniques de l'Ingénierie et de l'Innovation, 101 Antananarivo, Madagascar
3- Freelance, Scientific Consulting, SIRET N° (FR): 84872000900028, 92220 Bagneux, France

Corresponding author : Mbolanjara H. Andriamamonjy

Adress: Ecole Doctorale Ingénierie et Géosciences, 101 Antananarivo, Madagascar
e-mail : mbolanjarahelene@gmail.com

Phone number : +261 34 38 902 24

Abstract (< or = 250 words)

The analysis of the spatio-temporal distribution of aerosols, nitrogen dioxide (NO_2), formaldehyde (HCHO), and carbon monoxide (CO) in Madagascar is carried out considering several factors: fire phases and types of fuels burned. Savannah/grassland fires show a low fire radiative power (FRP) of 10 MW, while rainforests display an FRP greater than 100 MW. Early flame combustion generates significant emissions of NO_2 (10^{-4} mol/m^2), CO (4.10^{-4} mol/m^2) in the smouldering phase, HCHO (6.10^{-4} mol/m^2), and carbon aerosols (BC and BrC) with UVAI of 1.5. Smouldering combustion produces more CO and less absorbing organic aerosols (UVAI <0.5) or BC coated with OC. These pollutants, trapped in the atmospheric boundary layer (<3 km ASL), undergo physicochemical transformations under the influence of weather conditions including temperature and relative humidity. During the dry season, conducive to biomass fires, two types of pollution transport are observed. The first, on a regional scale, comes from the eastern regions causing a significant increase in $PM_{2.5}$ concentrations (120 µg/m^3) on 23 October 2023, in Antananarivo (and on 27 October), already continuously polluted by urban traffic. The second, on a larger scale, comes from South Africa bringing up to ~$8.06.10^6$ t of CO to the south of Madagascar on 18 October 2022. The use of satellite and surface observations, coupled with numerical modeling, proves to be important for advancing studies on air pollution and climate change related to aerosols and ozone (the SLCF) in Madagascar.

1- Introduction

Air pollution is a major public health problem in populated urban areas (https://www.who.int/fr/news-room/fact-sheets/detail/ambient-(outdoor)-air-quality-and-health , 2022), contributes to the deterioration of ecosystems and impacts agricultural production (IPCC, 2021). Along with the greenhouse gases (GHGs) released by anthropogenic activities worldwide, "SLCF = Short-Lived Climate Forcers" (cf. IPCC, 2021) also contribute to climate change and are classified as pollutants in the air quality sense. These include methane (CH_4), ozone (O_3), halogen compounds, nitrogen oxides (NO_x), carbon monoxide (CO), volatile organic compounds (VOCs), ammonia (NH_3), sulfur dioxide (SO_2) and aerosols composed of carbonaceous elements, organic and inorganic matter including, respectively, black carbon (BC), brown carbon (BrC), organic carbon (OC) and inorganic compounds including sulfate, nitrate and ammonium, sea spray and mineral dust. SLCFs are chemically reactive and participate in climate-related radiative processes; some produce ozone (coupling of CH_4, NO_x, CO and VOCs). Through human activity, SLCFs are simultaneously released along with the main GHGs. CO_2, N_2O, CH_4, O_3, NH_3 (and others) contribute to positive radiative forcing, and their increase leads to global warming. BCs absorb visible radiation (VIS) and generate warming, as do BrCs through UV absorption. OCs and inorganic aerosols, on the other hand, contribute to negative radiative forcing, resulting in global cooling. Aerosols are involved in the physical-chemical formation of clouds (condensation nuclei), whose role in climate change is of particular importance, especially for precipitation budgets and interactions with radiation (Konovalov et al., 2022 ;Tao et al., 2012). SLCFs have highly variable lifetimes, ranging from days to months and decades. BC, OC and O_3 have lifetimes ranging from days to weeks, CO months and CH_4 around ten years.

In addition to emissions of GHGs and SLCFs by human activities, the climate is also affected by so-called non-climatic factors, such as intensive farming and land-use change, including deforestation through forest fires and biomass fires, which alter the albedo of surfaces and produce a multitude of gaseous and particulate pollutants - a danger to human health and a determining factor in climate change. The work of the IPCC in 2021 reports that the contribution to global warming of some SLCFs (including CH_4, O_3 and BC) is +0.6 compared with that of CO_2 (+1.01°C), while the contribution of BrC has not been assessed. Climate change has multiple impacts on all sectors: environmental, economic, public health and social.

In terms of public health, numerous epidemiological studies have highlighted the relationship between air pollutants and various pathologies, notably for O_3, particulate matter (PM), NO_2 and HCHO (Olstrup et al., 2019; Kim et al., 2011). WHO recommendations for 2021 further restrict the maximum daily and annual thresholds for pollutants including $PM_{2.5}$.

In order to achieve the so-called "net-zero emission" transition in 2050, drastic reductions in SLCF emissions are essential worldwide (Raga et al., 2018; Allen et al., 2022). Sub-Saharan Africa, including Madagascar, are concerned via their Nationally Determined Contributions (NDCs).

Although Madagascar's main GHG emissions are well below those of developed countries, the country's SCLFs and non-climatic factors require a more in-depth and detailed diagnosis, accompanied by scientific research into monitoring and forecasting the state of air quality and climate. Madagascar is constantly under the influence of anthropogenic sources of emissions, and land use sources have yet to be assessed in detail. These sources include the importance and recurrence of biomass fires, forest fires (Andriamamonjy, 2022; Tahintsoa, 2018), land transport, open burning of agricultural and household waste, brickworks and charcoal production. Biomass fires are practised from April (early) to mid-December (before the rainy season) throughout the country, resulting in levels of pollutants such as $PM_{2.5}$ that exceed international standards (Aouizerats et al., 2015).

The SLCF emission inventories for Madagascar are either missing or incomplete and are fraught with uncertainties, for a variety of reasons. The effects of these sources and non-climatic factors on air quality and climate in Madagascar have also not been diagnosed, measured, monitored and explored using numerical pollution models. Ground-based measurement and monitoring networks and observations of the concentration and evolution of these pollutants in the atmosphere are inadequate for Madagascar.

Over the last few decades, the proliferation of polar-orbiting satellites for observing the earth and its atmosphere, carrying increasingly sophisticated and precise sensors with ever finer spectral resolution, has provided less advanced countries with long-term, wide-area observation data. Scientific research in Madagascar needs such databases to fill the gaps in its monitoring networks and measurements on the ground and at altitude. It is essential for the country to establish detailed and accurate inventories and emission registers of SLCFs from all anthropogenic and natural sources, using innovative methods published with the help of satellite observations, and to undertake scientific research into the monitoring, analysis and measurement of the characteristics and concentrations of SCLFs and their precursors. Numerical modelling work on chemistry-transport-radiation is making it possible to establish spatio-temporal distributions of SLCFs from the urban scale to the national scale, which are necessary for both climate and urban pollution studies. This work is already part of a research programme at doctoral (PhD) and MASTER level.

This work sets in motion the research programme listed above and focuses essentially, and for the first time in Madagascar, on detailed analyses of aerosol characteristics and SLCP concentration extracted from multiple satellite data. Data from MODIS Aqua and Terra, NOAA 20 and S-NPP VIIRS, Sentinel 2 L2A and 5P TROPOMI, Sentinel 3 SYN, CALIPSO and OMPS will be used. Extracted observations such as: UVAI, AOD, Angstrom Coefficient, Integrated Gas Column, are analysed according to the characteristics of the fires, their radiative power, the categories of fuel potentially burnt and environmental factors. For the urban case in Antananarivo, PM.5 is regularly measured using "low-cost" sensors, and processed with satellite data. Radio-sonde networks and global meteorological analyses are explored for the effects of parameters such as wind and the characteristics of the atmospheric mixing layer. In addition, the Hybrid Single-Particle Lagrangian Integrated (HYSPLIT) trajectory model is used to identify the origin or destination of a polluted air mass towards a specific area (Rolph, Stein and Stunder, 2017).

At the end of this work, and not covered in this article, the analysis results will make it possible to draw up more elaborate and detailed emission inventories of SLCPs and their precursors from fires and road transport, with new data on fire parameters, fuels and other characteristics, and to carry out multi-scale modelling of the distribution of pollutants using these databases, the results of which will be compared with satellite data.

3- Methodology

a) Study area

The analyses focus on the regional scale for all of Madagascar, on the local scale for isolated cases of forest fires in reserves and national parks, and for the city of Antananarivo. The selected areas are: Natural Integral Reserve of Tsaratanana (NIRT), Ankarafantsika National Park (ANP), Special Reserve Ambohitantely (SRA) and the city of Antananarivo with the districts of Alaotra-Mangoro (figure 1). In October, the average monthly temperature on the island varies between 20°C and 27°C; the season from September to November is a dry season conducive to the development of biomass fire practices for the island (Direction Générale de la Météorologie, 2014). However, 'early' fires appear from the month of April.

b) Satellite observation

The characteristics of the surface, aerosols (AOD, UVAI and Angstrom exponent) and NO_2, HCHO and CO are collected and analyzed from multiple satellite observations for specific days in October 2022. Sentinel 2, composed of Sentinel 2A and 2B, offers global coverage every 5 days in thirteen spectral bands, including four in the VIS and NIR channels at a very high resolution of 10 m, six bands at 20 m and three bands at 60 m. The successor to MODIS, Visible Infrared Imaging Radiometer is an instrument on board the Suomi National Polar-orbiting Partnership SNPP and NOAA-20. VIIRS uses 22 spectral bands with a resolution of 375 m and 750 m and observes the surface twice a day. Sentinel 2 with VIIRS is used to characterize fire intensity (Fire Radiative Power FRP) and top-of-atmosphere reflectance. This first instrument also allows to characterize vegetation types as well as burned areas. MODerate Imaging Spectroradiometer (MODIS) on board TERRA and AQUA, uses 36 spectral bands with spatial resolutions of 250m, 500m and 1km. The MCD19A2 product from MAIAC combines data from TERRA and AQUA to generate the aerosols optical depth (AOD) at a resolution of 1km and diurnal (Lyapustin et al., 2018). A compilation of MODIS AOD observations with Sentinel 3 will be brought in this study. Sentinel 3 (Sentinel 3A and 3B) combines the channels of the Ocean and Land Color Instrument (OLCI) and Sea and Land Surface Temperature Radiometer (SLSTR) to extract the AOD and Angstrom exponent at high resolution of 300 m for the SY_2_SYN product. The two Sentinel 3 satellites have a revisit time of less than two days for OLCI and less than one day for SLSTR (Optical Mission Performance Cluster, 2023). TROPOsheric Monitoring Instrument (TROPOMI) on board Sentinel 5 Precursor, makes daily measurements of various gases and parameters related to aerosol absorption in the UV, VIS, NIR and SWIR bands. It uses specific resolutions of 3.5 x 5.5 km^2 for NO_2 and HCHO and 5.5

International Journal of Engineering, Sciences and Technologies
ISSN : 3079-2045
https://www.ij-est.org/
Volume 2, issue 1, https://doi.org/10.70961/IKDY7329

x 7 km² for CO. In addition, UVAI is derived from the spectral absorption contrast in the UV for a given pair of wavelengths 340/380 nm and 354/388 nm (TROPOMI ATBD of the UV Aerosol Index, 2022). In combination with Sentinel 2 and TROPOMI observations, Ozone Mapping and Profiler Suite (OMPS), a suite of instruments on board the Suomi NPP and JPSS-2 satellites of NASA/NOAA, detects the aerosol index and FRP in the spectral bands in the UV and VIS. It flies over about 14 times a day with a resolution of about 50 km x 50 km at nadir. Finally, the CALIOP lidar from Cloud-Aerosol Lidar and Infrared Pathfinder Satellite Observations (CALIPSO) is a lidar that observes backscatters at 532 and 1064 nm. The 532 nm depolarization channel provides the vertical profile of aerosols with a horizontal resolution of 333 m and vertical resolution of 30 to 60 m for the altitude range between -0.5 km to 8.2 km (D. Winker et al., 2009).

c) Particulate matter $PM_{2,5}$ data

Daily concentrations of $PM_{2.5}$ provided by the Direction Générale de la Météorologie Madagascar are measured from 'low-cost Purple Air PA-II' sensors. These sensors use the technique of observing particles through laser optical counting. They then provide digital outputs of mass concentration fractions of PM_1, $PM_{2.5}$ and PM_{10}, cumulative distribution of particle size in six dimensions (>0.3 µm, >0.5 µm, >1 µm, >2.5 µm, >5 µm and >10 µm) and data on temperature, relative humidity and pressure (Tryner and al., 2020). It should be noted that in general, this type of instrument can only detect particles larger than 300nm.

d) Surface wind and trajectory model

Wind observation data at 0 UT and 12 UTC from FMMI Ivato were used to assess the impact of wind on pollutant distributions at local scale. In combination with these data, backward trajectory simulations of the Hybrid Single-Particle Lagrangian Integrated Trajectory (HYSPLIT) model were run to determine the origin of polluted air masses in a selected impact zone. In the HYSPLIT simulation, meteorological fields produced by NOAA's Global Forecasting System were chosen, with a temporal resolution of three hours and a spatial resolution of 0.25° (~31 km).

International Journal of Engineering, Sciences and Technologies
ISSN : 3079-2045
https://www.ij-est.org/
Volume 2, issue 1, https://doi.org/10.70961/IKDY7329

2- Results

a) General situation

Figures 2 a-b-c-d-e represent the general situation of the country in terms of: fires without exception, all satellites combined, characterized by their 'Fire Radiative Power' or radiative power-, respectively for the 3, 7 and 27 October 2022 with the iso-values of the UVAI of aerosols representing the absorbing organic compounds (340 nm and 380nm) (Buchard et al. 2015). These UVAI are extracted from the SNPP-OMPS satellite and marked in yellow range (source FIRMS). The burned areas in October 2022 are highlighted in neon green on figure 2-b. Figures d-e respectively display: the AOD, with a resolution of 1km2, extracted from the "MCD19A2 MODIS Deep Blue for Terra and Aqua Land Aerosol Optical Depth (AOD). Daily L2G Global 1 km. V6.1" database. On 18 October 2022, the corresponding UVAI extracted from SENTINEL 5P TROPOMI (S5PTR) at the same passage times are presented in (e). The intensity of the fires is materialized by their FRP in MW. For the blue ranges, the FRP are around 10MW, in green >50MW and in red > 100MW. By comparison between MODIS and VIIRS, Li et al., 2018, showed that cultivated lands display FRP (fire groups) with a maximum of 400MW, humid tropical forests of 1000MW, savannas of 1500 MW and deciduous forests of 35000MW. In Madagascar, these ecosystems are present and the FRP parameter remains a good essential indicator for the calculation of emission factors and the analysis of pollutant distribution. On the island, the values of the FRP, derived from these satellites, vary according to the regions, depending on several factors, including burning conditions (flaming or smoking), types of biogenic fuels (dense forest wood- gallery forests, grassy meadows, shrubs of the maquis, grass-shrubs of savannas, agricultural waste, etc.), i.e. the type of burned ecosystems and their conditions (dry-humid forests, soil water content). With the practice of "tavy", the meadows correspond to lower FRP compared, and this in order of importance, to the burning of shrub fires in the maquis (the most significant), dense forests and agricultural waste (cf. Palumbo et al., 2011). The emission factors of gases and aerosol components partly depend on these multiple factors and data.

A frontal system observed on 03 October in the south of Madagascar and fires in the Southeast regions of Africa, moves north to cross and cover more than half of the country. On 07 Otober, another front is found. These frontal systems advect towards Madagascar, layers of aerosols and gaseous pollutants like CO, produced by fires in Africa. This pollution is materialized by layers at altitude (in yellow) and positive UVAI reaching the Northwest of the island on 25 October and dissipating on 27 October (figure 2-c).

International Journal of Engineering, Sciences and Technologies
ISSN : 3079-2045
https://www.ij-est.org/
Volume 2, issue 1, https://doi.org/10.70961/IKDY7329

On 18 October the AOD from MODIS show values between 0.4 and 0.6 in the great South, partly linked to large-scale advection, from 0.2 to 0.4 in the central South and values <0.2 in the Northwest ; the presence of clouds prevents the extraction of AOD (white area). The general distribution of UVAI shows values linked to “young” emissions from fires with values between 0 and 1.4, characteristic of absorbing organic aerosols (BrC). On 18 October, the great South, the central South, the Northwest and part of the center display marks of presence of BrC; the eastern part being covered by clouds, the interpretation is to be nuanced. The central part of the country presents areas weak in BrC certainly after oxidation and loss, quite rapid of these organic aerosols. On a finer scale, in the fire zones, the AOD exceed 0.8.

Two passages of the CALIPSO satellite carrying a CALIOP LIDAR, classifying aerosols along its orbit, have shown their profile in figures 3 (a-b-c-d). The aerosol layer present in the Southeast of Africa (figure 2-b) on the island on 07 October, is found in the aerosol profile (black area) reaching 5km ASL. This transport and mixing of aerosols in the atmospheric boundary layer (ABL) have an impact on the values of the extracted AOD and those of $PM_{2.5}$ at the surface. On the other hand, for 18, CALIPSO shows an aerosol layer (in light brown) not exceeding 3km ASL for all of Madagascar. For a very large majority of CALIPSO passages in October 2022, the aerosol layers are located below 3km ASL; data supported by the potential temperature profile in radiosondes at the Ivato (FMMI) station.

b) Case studies

A few case studies across the country, at the local and regional scale and urban for Antananarivo (with $PM_{2.5}$ at the surface), explore and analyze the distribution of fire emissions including aerosol characteristics (UVAI, AOD) and the integrated column of pollutants NO_2, CO, HCHO, in the plumes and far away from the fire zones. These analyses focus on the horizontal (sometimes vertical) distribution and evolution of pollutants and aerosols in the vicinity of near and far fires and, for Antananarivo, on the impacts on air quality by superimposition with car traffic emissions. These studies are essential for the spatio-temporal estimation of pollutant emission rates at these scales, to feed the inputs of numerical models calculating the distribution of pollutants, followed by a comparison with satellite observations.

i. Case study 1: Ankarafantsika National Park (ANP) and surrounding area

ANP is located in the Boeny region between the town of Marovoay and Ambato Boeny, bounded to the east by the Majahamba river and crossed by the RN4. The park is made up of dense primary forests, dry forests (https://whc.unesco.org/fr/list/494/) and savannahs. The area

INTERNATIONAL JOURNAL OF ENGINEERING, SCIENCES AND TECHNOLOGIES
ISSN : 3079-2045
International Journal of Engineering, Sciences and Technologies
ISSN : 3079-2045
https://www.ij-est.org/
Volume 2, issue 1, https://doi.org/10.70961/IKDY7329

to the south of the park, bordered by the Boeny administrative boundary, is partly made up of hectares of rice paddies.

Figures 4 a and b show respectively: (a) the ANP area observed by Sentinel 2 L2A (S2L2A) on 25 September 2022 at 07:15 UTC in the SWIR band, the day before the fires started, when the vegetation was still flamboyant, and (b) the progression of burnt areas (SWIR in brown) on 30 September with fire outbreaks.

Figure 4 c shows in white the accumulated burnt areas for the month of October 2022, where fires mainly concerned the park's forests - or savannahs - and, in yellow, the same areas for the month of April 2022, where fires were most likely set to burn agricultural waste in the rice fields. In fact, according to these satellite observations, the first fires in the southern zone of the ANP start and end in April (end of harvests?), become rare in the following months and reappear in October, this time in the ANP. In Figures 5 a and c (SWIR) and b) (visible), the observations show a clear progression of the burnt areas on 10 October (a) when a maximum of fire emissions (with the day of 11 October), is analysed for gases and aerosols. The fire fronts reached a spread of 1.5km to 2km. Smoke is visible (b), showing the smouldering appearance of the fires and their flamboyant appearance, which are essential indicators for differentiating pollutant emission factors.

20 October represents the beginning of the end of the fires (reached on 25 October), shown in figure 4-c. The entire area in brown (SWIR) is burnt during the fire period, which was intermittent but active for 30 consecutive days in October 2022.

Figure 6a shows the reflectance observed by S-NPP VIIRS (source NOAA) on 10 October at 10h15TU with FRP>>100MW at the outbreaks (red pixels); the most active day of the period in terms of fire intensity. This situation is observed 3 hours after the passage of S2L2A at 07h15TU, shown in Figure 5b. In other areas of the park (pixels in brown), S-NPP VIIRS detects fires of lesser intensity - brown zone - with 35MW <FRP <100MW, either fires in the smouldering phase or another flaming ecosystem but with less energy. The Google Earth map of the ANP (not shown here) shows that the fire zones correspond to the dense forests within the park and their edges -potential clearing-; a diagnosis of the type of biogenic fuels is essential for a reassessment of the emission factors at these scales and in these locations. Figure 6b shows the same S-NPP VIIRS observations on 11 October for comparison of AOD in the following paragraphs.

The observations extracted from the S5PTR satellite (UV and SWIR) allow detailed analyses of the distribution and evolution of pollutants (gases, aerosols) in the plumes and around the distant zones under the plume. For all the observation and extraction bands for NO_2, HCHO

International Journal of Engineering, Sciences and Technologies
ISSN : 3079-2045
https://www.ij-est.org/
Volume 2, issue 1, https://doi.org/10.70961/IKDY7329

and UVAI, the current spatial resolution of the pixels is 3.5km by 5.5km and for CO extraction (SWIR) 7km by 5.5km. The daily distribution of AOD at 1km resolution is compiled from the MCD19A2 database (https://lpdaac.usgs.gov/products/mcd19a2v061/).

Figures 6 c and d show respectively the distribution of AOD on 10 October and 11 October from MODIS AQUA at 10:35 UT. Although the plumes of smoke observed by VIIRS have a similar expansion on the two previous days, the AOD show very different distributions with a notable expansion on 10 October and the appearance of slightly more polluted areas. An enlarged area with AOD of 0.2 to 0.4 on 10 October, occupying all of half the ANP area, with another range of 0.4 and 0.6 in the centre of the plume.

The area to the south of the ANP was polluted by aerosols on 10 October due to the appearance of other local fires (observations by other satellites on FIRMS not shown). It was the smouldering aspect of the aerosols that took precedence on 11 October. Figures 7 a-b-c-d show the respective distributions of UVAI, integrated NO_2, CO and HCHO contents on 10 October 2022 as S5PTR passed overhead at 09h50TU and e-f-g-h the same observations on 11 October. On 10 October, the intensity and number of fires (cf. Figure 5a) led to the presence of a zone of larger BrC aerosols with UVAI max=1.5 (a), whereas on 11 October, the fires slowed down and the UVAI values were low (max 0.3). On 13 October (not shown), in the same zone of the less frequent fire plumes, the UVAI reached values relating to non-absorbent aerosols, which can be interpreted a priori by the fact that the lifetime of the BrCs in these zones does not exceed one day. NO_2 is an indicator of the intensity of the flames as it is produced by the rapid oxidation of NO. On 10 October, two main fire outbreaks were observed by all the satellites in the ANP, followed by a maximum of NO_2 well in excess of 10^{-4} mol/m^2 over a very large area (b), while on 11 October, this maximum was 6.5 10^{-5} mol/m^2.

Due to its shorter lifetime, NO_2 remains confined to the vicinity of the fire fronts. CO shows the same characteristics and variations for the same dates (c) and shows almost a factor of 2 reduction in content between 10 and 11 October but is more widespread. CO is a product of incomplete combustion of smouldering fires and is more mixed and diffused in the atmosphere because of its longer lifetime. HCHO is also a product of biogenic combustion. Once emitted, HCHO is photodissociated, reacts chemically with NO and OH and participates in the formation of NO_2 and ozone (greenhouse gases). Its somewhat chaotic spatial distribution is linked to this photochemical reactivity, which depends on the seasons. For the ANP with its burnt ecosystems, when the fires are in the flamboyant phase and more numerous, emissions of gaseous species are greater, with AOD remaining <0.4. On the other hand, during the smokier phase (11 October), the aerosol content increases sharply while dispersing to cover larger areas. During

International Journal of Engineering, Sciences and Technologies
ISSN : 3079-2045
https://www.ij-est.org/
Volume 2, issue 1, https://doi.org/10.70961/IKDY7329

the off-season (beginning of the dry season in April 2022), spatially scattered fires of agricultural waste in the rice fields to the south of the ANP were observed; the concentrations of all the species and the AOD were much lower than in October 2022. These analyses are consistent with certain conclusions reached in the studies by Palumbo et al. in 2011 for the FRP of agricultural fires.

ii. Case Study 2: Tsaratànana Integral Nature Reserve (DIANA)- NRIT

The NRIT, a protected area, consists mainly of dense rainforest with evergreen trees, is locally humid and subject to abundant rainfall, and has a short dry season. Ericoid scrub colonises the higher altitudes. The NRIT was hit by forest fires seen by satellite starting on 25 September 2022 and ending on 26 October 2022, i.e. lasting 30 days as for the ANP. During this period, the days of 7, 8 and 9 October were among the most intense in terms of crescendo fires. Figure 8a shows a detailed example of the degradation of ecosystems in the NRIT (Google Earth), most likely including multiple, non-limitative categories such as the exploitation of wood and land through deforestation and slash-and-burn. Figures 8 b and c show an episode of 3 simultaneous aligned fire outbreaks on 7 Ocotber, observed by S2L2A (True Color and SWIR) with smoke plumes spreading over a distance of more than 30km. The SWIR observations (c) show clearly visible flame fronts. In figure (d), the F1 focus is 2km by 2km, the 2nd F2 is 1.5km by 1km and the 3rd is 650m by 650 m; all 3 are in the "blazing fire" phase according to the SWIR image in these figures. These specificities linked to the type of fuel are unique and have a consequence on the rate of pollutant emissions.

On 7 October at 09:32 UTC, S-NPP VIIRS detected a plume of smoke (Figure 9a) reaching the ocean over 250km in length and passing over the town of Ambanja and the surrounding area (Figure 9a), while MODIS confirmed, already at 07:00 UTC (Figure 8b), the expansion of the same plume with maximum AOD of 0.8 at the focal points.

At a much finer resolution of 330m with Sentinel 3 Synergy (instead of 1km with MODIS), over land, the aerosol content thickened and occupied more surface area from 07 to 8 October and 9 October (figure a-b-c) - taking into account the colour scale effects with 07 October. On 7 October (a), with less intense and less developed fires (3 outbreaks), areas with AOD between 0.4 and 0.6 were located around the outbreaks, while maxima of 0.8 were observed at the flame fronts. On 08 October (b), the content thickened further and the maximum now reached 1.1 with values of 0.8 in the distant plume. On 09 October (c), the plume with AOD=0.8 covered a very large area, with a maximum of 1.5 in the vicinity and centre of the outbreaks, a situation linked to the number of larger fires in the NRIT and their intensity (FRP).

The S5PTR observations are shown in Figures 11 a-b-c-d-e. (a) corresponds to the UVAI on 07 October, the plume of which is expanding over more than 250km (figure 8a and b), within which the UVAI of the BrCs are between 1.3 and 3 (compared with the UVAI at ANP of 1.4). On 9 October, the content of these aerosols became more pronounced, with UVAI of 5 in a large part of the plume (Figure 11b). On 8 October, according to data extracted from Sentinel 3 SYN, the AOD at 550nm corresponded to an Ångström coefficient of 1.08 in the plume of 8 October in the vicinity of the outbreaks (data to be confirmed). This value of the coefficient could result from the mixing of aerosol types, in this case BC and BrC, in the plume. The value very close to 1 is characteristic of BCs (theoretical) whose absorption is independent of wavelength. Russel et al, 2010 published values of 1.3 for wavelengths between 440nm and 870nm for fires in savannahs in southern Africa. For NRIT, the fuel consists of forest wood.

With the FRP observed by S-NPP VIIRS and the number of flaming fire fronts, the integrated NO_2 content around the centre of the outbreaks, in the flame fronts, shows maxima well > 10-4 as in the case of ANP. The CO content at NRIT on 09 October was well in excess of 10^{-1} mol/m^2 (at ANP: max CO >= 4.10^{-2} mol/m^2). These higher concentrations and emissions of NO^2 (high temperature, blazing fires) and CO (smoking) are correlated with several data from the NRIT ecosystems, including the type of wood fuel and humidity. Figure 11e shows the integrated HCHO column on 09 October, which is shown for information purposes since the AQ is low. For most fire days in the NRIT, its distribution is not chaotic like that of the ANP; its concentration is highest around the centre of the fires. The presence of a few clouds, which limit its photodissociation, as well as higher humidity outside the fire zones, could influence its chemical reactivity and evolution and shorten its lifetime, hence the confinement around the centres. However, this hypothesis remains to be verified by modelling. As a first conclusion, the types of ecosystems and their conditions, as well as the external environment of the NRIT, partly explain the aerosol distributions and their characteristics, and those of the gases and above all the significant quantity of emissions. The NRIT has experienced intense fire-related events.

iii. Case study 3: Ambohitantely Special Reserve - SRA- within the Tampoketsa Plateau

The SRA covers an area of 5,800 ha, including 3,800 ha of grass savannah and 1,800 ha of natural forest. It is located on the high plateaux of Tampoketsa and appears to be tiny compared with the large areas of the plateaux. The interest of this analysis lies in the specific geographical situation of the SRA, the plateau ecosystems and the recurrent fires in the region, shown by way of example in Figure 12a. There are large undulating areas of grassland on lateritic soils, green river thalwegs in the hot season, gallery forests and a few secondary eucalyptus forests. These ecosystems are regularly subject to human fires: for grazing ("tavy"), for slash-and-burn cultivation, fires in eucalyptus (charcoal) and pine forests; the SRA is no exception to these practices.

Figure 12 b shows the outbreaks of fire in the SRA during the passage of S2L2A on 12 October 2022 at 07:05 UT (no passage of S2L2A on 11 October). Small flame fronts can be seen at the edge of the forests within the SRA, and the areas already burnt before this date are shown in brown. The corresponding plume of smoke, 10km across, seen by S-NPP VIIRS on 11 October, extends up to 80km under the effect of a south-easterly wind. In a wider field, Figure 13a shows the reflectance seen by NOAA20 - VIIRS on 11 October at 10:45 UT with the FRP values. NOAA20 VIIRS detected a few fires scattered over the plateaux, particularly between the SRA and the Ambohijanahary reserve to the west (dense forests); other satellites may also detect other fires on the same day (see FIRMS). The UVAI for the day (BrC), extracted from S5PTR on 11 October at 10:00 UT, show values of 0.6 for the SRA and more than 1.4 for Ambohijanahary (forests). On the Tampoketsa plateaux between the 2 reserves, despite the scattered fires, the aerosols tend to be less absorbent organic compounds (cyan colour) or the environment remains without any absorbent aerosols at all (blue zone). This situation is consistent with the AOD on the Tampoketsa plateaux (Figure 14a), whose distribution remains quite uniform: in the north between 0.2 and 0.4 and in the centre very low < 0.2. The Ambohijanahary reserve has AOD of 0.4 to 1 around the outbreaks. The plume of smoke from forest fires, which is fairly limited in size in the SRA (Figure 14 b), shows AOD of between 0.4 and 0.6 and some areas of 0.8.

The S5PTR observations are shown in Figures 15 a-b-c. On 11 October the BrCs displayed UVAI values of only 0.6 (fairly low) and this situation persisted until 12 October (smouldering fires with a few flame fronts). On 13 October (figure not shown), in the absence of fires, the absorbing BrCs completely disappeared from the plume residue and the surrounding area, if the corresponding UVAI values are anything to go by, indicating a lifetime of less than a day. NO_2 displays values similar to those observed at the ANP on 11 October but does not reach the maxima at the ANP on 10 October (flamboyant). The same situations were observed for CO. In conclusion, during the fire period, the SRA had lower emissions than the forests at the ANP and the NRIT; the type of ecosystems at the SRA certainly contributed to this difference under the additional effect of the environment such as the dry and windy climate.

iv. Case study 4: Antananarivo and the surrounding area

Antananarivo, with a surface area of 86km₂, is the capital of Madagascar, where most energy-intensive economic activities take place. According to INSTAT in 2018, the population density is 35,000 inhabitants/km^2. The city's road transport system consists mainly of highly polluting second-hand vehicles (private, public, heavy goods vehicles, 2-wheelers), a high proportion of which are between 10 and 40 years old (personal research). The number of cars on the road and the road system are the main sources of gaseous and particulate pollutants in the city. The Direction Générale de la Météorologie (DGM) has measured the concentration of fine particles $PM_{2.5}$ by installing "low-costs Purple Air PA-II" sensors at several locations in the capital along a very busy road (P1, Soanierana, south of the city centre) and at the DGM (to the north-east, P2) near a fairly busy road located high up and 5km from P1. Analyses of the data for the winter and warm seasons showed that the monthly averages for $PM_{2.5}$ in October (with fires) were twice those in May (without fires), linked to emissions from recurring biomass fires, which accumulate with emissions from urban transport in October. Episodes of $PM_{2.5}$ pollution were observed throughout October 2022, except on one day: 31 October, which did not exceed 15 $\mu g/m^3$ (WHO- 2021 threshold). The day of 7 October represents one of the many interesting cases to be analysed with $PM_{2.5}$ measured on the ground, satellite AOD and gases.

- Case of 07 october 2022

The concentration of $PM_{2.5}$ at the 2 stations P1 and P2 showed daily averages of 70 $\mu g/m^3$ (P2) and 75 $\mu g/m^3$ (P1) respectively, i.e. 5 times the WHO threshold (383%). The corresponding AOD values, extracted from the MODIS-MAIAC databases, are 0.65 (P2) and 0.4 (P1). The wind direction is 120° and the intensity 15kt (fairly high). In general, the daily AOD for the month at the 2 stations are of the same order of magnitude, so the average of the 2 is adopted here. These pollution peaks can be explained by the following situations. Figures 16 a-b show respectively the reflectance and the FRP of the fires seen by S-NPP VIIRS on 7 October at 11h10TU and the distribution of the AOD by MODIS at 07h00TU.

The plumes are now developed with S-NPP VIIRS views. The plume from the fires at Antsaranambe (a) has reached the city of Antananarivo with FRP well in excess of 100MW, amidst other smaller plumes. At 07:00UTC, MODIS had already detected these plumes with AOD >>1 in the centre of the Antsaranambe plume. For the others, the AOD remain around 0.4. In reality, the fires started on 6 October but remained confined around the outbreaks. The CALIPSO satellite was able to detect the aerosol profile (figure not shown) whose peak reached 5km ASL, which explains the AOD values of 0.65 at P2, accompanied by high $PM_{2.5}$ values measured on the ground.

International Journal of Engineering, Sciences and Technologies
ISSN : 3079-2045
https://www.ij-est.org/
Volume 2, issue 1, https://doi.org/10.70961/IKDY7329

Figures 17 a and b show the correlation between $PM_{2.5}$ and AOD on 07 October, (a) for all days in October at P2 and P1 with $PM_{2.5}$/AOD ratios between 113 and 836. As a reminder, the average MODIS AOD value between P1 and P2 is 0.5. and (b) for a selection of pairs of values for dates where the ratios are less than 200, a threshold which seems to us to be "reasonably uniform" in terms of the relationship between the 2 entities. This "selection" improves the correlation coefficient (R^2= 0.77 instead of 0.39 for all ratios) between $PM_{2.5}$ on the ground and satellite AOD during the fire period and under heavy pollution in October. This type of larger-scale analysis is very useful for the future, at least for establishing a $PM_{2.5}$ concentration using AOD in the absence of ground-based sensors, coupled with in-depth analyses of the other radiative characteristics of aerosols, their mixing state in the atmospheric boundary layer, and their size and composition distribution.

Observations extracted from Sentinel 5P TROPOMI are shown in Figures 18 a-b-c-d for 7 October 2022 for a passage around 10h50 UT. (a) shows a plume of absorbing organic aerosols with a relative content at a maximum of UVAI =1.4. The wind blowing from 120° and from 9 to 15 kt between 00 UT and 12 UT on 7 October caused this tongue of "BrC" to spread across a smaller area than the plume of CO (c) and even NO_2 (b), whose maximum 4.10^{-4}mol/m^2). This additional pollution - superimposed on the emissions from car traffic in the city - still results in a $PM_{2.5}$ level of 75 µg/m^3 (P1- 5X the WHO threshold) despite the 15 kt-120° wind intensity at the surface. This concentration is admittedly lower than the 120 µg/m^3 measured on 23 October (P1) but the wind was 4kt up to 3km ASL, the height of the mixing layer observed by FMMI, so less dispersion. The distribution of chemically reactive HCHO in the plume, in the presence of sunlight and other chemical species (NO_2, OH, O_3). Despite this, an HCHO bubble was observed over the city of Antananarivo, but it remains to be seen whether this is partly linked to the smoke plumes at Antsaranambe or simply local emissions.

In conclusion, this work has not been able to show all the events of pollution by fires coupled with emissions from automobile transport in the city of Antananarivo in the month of October 2022 every day. However, following the example of 7 October, the recurrent very active period, from year to year, of fires in the Analamanga, Alaotra-Mangoro and Atsinanana regions (east of the city), in October and November, with an average wind from the east, results in $PM_{2.5}$ pollution levels 3 to 8 times (exceptional case) the WHO recommendation threshold during these months. In October 2022, only the date 31 October measured a daily concentration of $PM_{2.5}$ = 15 µg/m^3, and in November 2022, no date. Two months of acute rather than chronic low-level exposure of the population to $PM_{2.5}$. In June 2023, without the influence of biomass fires, only 4 days did not exceed 15 µg/m^3 in Antananarivo, whereas WHO recommendations for the number of polluted days stipulate not exceeding 3 to 4 days per year (99th percentile). Thanks to the presence of PM2.5 sensors and satellite observations, the city of Antananarivo offers a number of advantages for more elaborate and comprehensive short- and long-term studies of the effects of emissions from fires and cars. However, in addition to aerosols and particles, it is essential to add ground-based gas sensors such as SLCFs (Short-Lived-Climate-Forcers) and other precursors, and to carry out numerical modelling.

c) Large-scale transport of pollutants from fires in South-East Africa

Every year, East Africa is subject to large-scale biomass fires, such that, linked to atmospheric circulation to the south of Madagascar and over the Mozambique Channel (Sinha et al., 2004), exchanges of fire-polluted air masses between Africa and Madagascar have been observed for years by successive satellites such as MOPITT, MODIS and Sentinel 5P. To analyse the impact of air mass incursions from the south-east of the continent, certain days in October 2022 are compared, in the CO column extracted from Sentinel 5P TROPOMI, to a reference day with no African air mass incursions, i.e. 30 October 2022. The differences between the distribution of CO from 16 to 20 October and that of 30 October are shown in Figures 19 a-b-c. On average, the air masses contain a difference in CO content of 0.02 to 0.04 mol/m^2. For the days from 16 to 20 October, emissions from biomass fires in southern Africa, transported by the passage of a frontal system, moved from south to north and then eastwards to cover the large southern half of Madagascar.

The evolution of the plume is very visible between 16 and 18 October and reaches its maximum influence on the country between 18 and 20 October. These two days represent examples of the incursion of pollution from biomass fires in Africa onto the Grande Ile. The large plume then dispersed northwards on a regional scale, gradually dissipating the CO incursion before becoming invisible on the satellite observation of 20 October.

During these periods, the Hysplit backward -trajectories show air mass lifting above the atmospheric boundary layer on 17 October, followed by eastward advection. A dominant south-westerly flow between 3000 m and 5600 m ASL favours the movement of this polluted air mass towards Madagascar. According to this simulation with HYSPLIT, this flow of additional CO concentration from the African soil observed by Sentinel 5P TROPOMI S5P constitutes part of the column of aerosols observed by CALIPSO around these dates over the southern half of the large island. As each incursion brings with it a mass of pollutants, statistical studies of these phenomena to establish a mass balance will require the use of more sophisticated 3d chemistry and transport models, followed by a more or less long-term forecasting model.

3- Discussions

This in-depth study of air pollution in Madagascar highlights the complex correlations between emission sources, local ecosystems and meteorological conditions. In October, analyses of isolated cases reveal specific emissions of pollutants in different areas of the island, influenced by the various ecosystems. Biomass fires are the main source of emissions, with intensities varying according to the type of fuel burnt.

The results detail the significant emissions of BrC, NO_2, CO and HCHO during blazing fires in the dense forests of the ANP, showing a variation in the combustion phases. The differences observed at NRIT compared with ANP highlight the influence of factors such as humidity on emissions and chemical transformations of gases. At regional level, SRA has relatively low emissions due to differences in biomes and the dry climate of the highlands. Antananarivo, on the other hand, experiences pollution peaks linked to local emissions, accentuated by biomass fires and meteorological conditions favourable to the stagnation of pollutants.

The study also highlights the impact of Africa on air quality in Madagascar, with smoke advection at high altitude. Satellite observations are proving crucial for quantifying and monitoring changes in pollutant emissions and concentrations across the island.

However, questions remain, notably the need for a detailed classification of biomes and the integration of complementary methodologies, such as the top-down approach, for a complete understanding of pollution in Madagascar. Urgent research prospects include the development of comprehensive inventories of short- and long-lived pollutants, exploiting recent methodological advances and new generations of satellite instruments. These databases will be essential for feeding numerical models and assessing the impacts of aerosols and precursors on health and climate in Madagascar, underlining the importance of taking a holistic approach to tackling air pollution problems on a regional scale.

4- Conclusions

Our study of the distribution of aerosols and gases in Madagascar in 2022 revealed significant trends. Biomass fires in eastern Madagascar have led to a significant increase in pollutant concentrations in Antananarivo, sometimes exceeding WHO thresholds, putting public health at risk. On a regional scale, smoke emissions showed marked correlations with high concentrations of aerosols and trace gases, favoured by calm wind conditions. Biomass fires in southern Africa significantly influenced carbon monoxide concentrations in eastern Madagascar.

These results underline the crucial importance of satellite observations for quantifying emissions and establishing correlations. Future research prospects include the development of advanced dispersion models to better anticipate the spread of pollutants, an in-depth understanding of local and regional emission sources with a view to implementing targeted mitigation policies, and the exploration of the climatic implications of high concentrations of greenhouse gases and fine particles, including their interactions with other climatic parameters. These areas of research are essential for improving air quality, protecting public health and helping to fight climate change in Madagascar.

5- Acknowledgements

We would like to thank the Service de Recherches Hydrométéorologiques within the Direction Générale de la Météorologie Madagascar for providing us with the fine particle concentration data measured by the sensors Purple Air. The authors would also like to thank NASA, NOAA, CNES, EUMETSAT and ESA researchers for making the data of Sentinel 2, Sentinel 3, VIIRS, MODIS, Sentinel 5P TROPOMI, OMPS and CALIPSO available. For TROPOMI, Copernicus Sentinel data [2022] for Sentinel data contains modified Copernicus Sentinel data [2022] for Sentinel data. We would also like to express our gratitude to the scientists at the NOAA laboratory for providing the HYSPLIT model used in this pubication. The authors would like to thank all the people who contributed to this work: Nomenjanahary Lovasoa Sarobidy for the AOD data extractions and all the reviewers for their valuable feedback. This work was based on the master thesis of Mbolanjara H. Andriamamonjy.

6- Références

Ahmed El Nemr ,« Impact, Monitoring and Management of Environmental Pollution ».2010.

Ahmed El Nemr, « Environmental Pollution and its Relation to Climate Change ». 2011.

Allen, M. R., Peters, G. P., Shine, K. P., Azar C., Balcombe P., Boucher O., Cain M., Ciais P., Collins W., Forster P. M., Frame D. J., Friedlingstein P., Fyson C., Gasser T., Hare B., Jenkins S., Hamburg S. P., Johansson D.J. A., Lynch J., Macey A., Morfeldt J., Nauels A., Ocko I., Oppenheimer M., Pacala S. W., Pierrehumbert R., Rogelj J., Schaeffer M., Schleussner C.F., Shindell D., Skeie R. B., Smith S. M., Tanaka K. Indicate separate contributions of long-lived and short-lived greenhouse gases in emission targets. *Clim. Atmos. Sci*. 2022. https://doi.org/10.1038/s41612-021-00226-2

Andriamamonjy, M. H. Étude de la distribution des aérosols, liée aux feux de la biomasse à Madagascar Madagascar par observations satellitaires. 2022. Engineering thesis, Ecole Supérieure Polytechnique d'Antananarivo, Department: Météorology.

Aouizerats, B., van der Werf, G.R., Balasubramanian, R., Betha, R. Importance of Transboundary Transport of Biomass Burning Emissions to Regional Air Quality in Southeast Asia During a High Fire Event. *Atmos. Chem. Phys 2015*. doi:10.5194/acp-15-363-2015.

Buchard, V., da Silva, A. M., Colarco, P. R., Darmenov, A., Randles, C. A., Govindaraju, R., Torres, O., Campbell, J., and Spurr, R.: Using the OMI aerosol index and absorption aerosol optical depth to evaluate the NASA MERRA Aerosol Reanalysis. 2015. *Atmos. Chem. Phys.,* 15, 5743–5760, doi:10.5194/acp-15-5743-2015.

Direction Générale de la Météorologie, Atlas climatologique de Madagascar, (2014).

Giglio, L., Schroeder, W., & Justice, C. O. (2016). The collection 6 MODIS active fire detection algorithm and fire products. *Remote Sens. Environ.*, 178, 31–41.

IPCC (Intergovernmental Panel on Climate Change). *Chapter 6, Short-lived climate forcers.* 2021.

Ivar R. van der Velde, Guido R. van der Werf1, Sander Houweling,, Henk J. Eskes, J. Pepijn Veefkind, Tobias Borsdorff2, and Ilse Aben, Biomass burning combustion efficiency observed from space using measurements of CO and NO_2 by the TROPOspheric Monitoring Instrument (TROPOMI). *Atmos. Chem. Phys*., 21, 597–616, 2021. https://doi.org/10.5194/acp-21-597-2021.

Khaled Chetehouna ,« Volatile Organic Compounds: Emission, Pollution and Control ». June 2014.

Kim K-H., Jahan S. A., Lee J-T. Exposure to formaldehyde and its potential human health hazards. *J. Environ. Sci. Health C Environ. Carcino.g Ecotoxicol. Rev. 2011, 29*(4), 277–299, doi: 10.1080/10590501.2011.629972.

Konovalov I. G., Golovushkin N. A., Beekmann M., Turquety S. Using Multi-Platform Satellite Observations to Study the Atmospheric Evolution of Brown Carbon in Siberian Biomass Burning Plumes. *Remote Sens. 2022, 14*(11), 2625. https://doi.org/10.3390/rs14112625.

Li, F., Zhang, X., Kondragunta, S., & Csiszar, I. Comparison of fire radiative power estimates from VIIRS and MODIS observations. 2018. *Journal of Geophysical Research: Atmospheres*,123,4545–4563 https://doi.org/10.1029/2017JD027823.

Lyapustin, A., Wang, Y., Korkin, S., and Huang, D.: MODIS Collection 6 MAIAC Algorithm, Atmos. Meas. Tech., 11, 5741-5765, https://doi.org/10.5194/amt-11-5741-2018, 2018.

Maurits L. Kooreman, Piet Stammes, Victor Trees, Maarten Sneep, L. Gijsbert Tilstra, Martin de Graaf, Deborah C. Stein Zweers, Ping Wang, Olaf N. E. Tuinder, and J. Pepijn Veefkind, Effects of clouds on the UV Absorbing Aerosol Index from TROPOMI, *Atmos. Meas. Tech.,* 13, 6407–6426, https://doi.org/10.5194/amt-13-6407-2020, 2020.

Olstrup H., Johansson C., Forsberg B., Åström C. Association between Mortality and Short-Term Exposure to Particles, Ozone and carbone dioxide in Stockholm, Sweden. *Int. J. Environ. Res. Public Health 2019, 16(6), 102*, DOI: 10.3390/ijerph16061028.

Optical Mission Performance Cluster , Copernicus Sentinel-3 SYN Land User Handbook, 2023, OMPC.ACR.HBK.003.

Palumbo I., Grégoire J.-M., Simonetti D. and Punga M., Spatio-temporal distribution of fire activity in protected areas of Sub-Saharan Africa derived from MODIS data. 2011. *Procedia Environ. Sci.*, Volume 7, 2011, Pages 26-31.

Prashant Kumar,« Airborne Particles: Origin, Emissions and Health Impacts ». June 2017.

Raga G. B., Kuylenstierna J., Claxton R., Shindell D., Foltescu V., Cong H., Borgford-Parnell N. Addressing black carbon emission inventories, A report by the climate and clean air coalition scientific advisory panel. Climate & Clean Air Coalition to Reduce Short-Lived Climate Pollutants. 2018.

Russell, P. B., Bergstrom, R. W., Shinozuka, Y., Clarke, A. D., De-Carlo, P. F., Jimenez, J. L., Livingston, J. M., Redemann, J., Dubovik, O., and Strawa, A.: Absorption Angstrom Exponent in AERONET and related data as an indicator of aerosol composition. 2010. *Atmos. Chem. Phys.,* 10, 1155–1169, doi:10.5194/acp-10-1155-2010.

Sinha P., Jaegle L.´, Hobbs V. P. and Liang Q. (2004), Transport of biomass burning emissions from southern Africa, *J. Geophys. Res.*, Volume. 109, D20204, doi:10.1029/2004JD005044.

Stein A. F., Draxler R. R., Rolph G. D., Stunder B. J. B., Cohen M. D., Ngan F. NOAA's HYSPLIT atmospheric transport and dispersion modeling system. *Bull. Am. Meteorol. Soc 2015,* 2059-2077, DOI: https://doi.org/10.1175/BAMS-D-14-00110.1.

Tahintsoa, G. H. Analyse spatiale et intra-annuelle des surfaces brulées à partir des images Modis en vue d'améliorer la gestion des ressources naturelles à Madagascar. *2018.* Engineering thesis, Ecole Supérieure des Sciences Agronomiques, Department: Foresterie et Environnement.

Tao W-K., Chen J-P., Li Z., Wang C., Zhang C. Impact of aerosols on convective clouds and precipitation. *Rev. Geophys. 2012, 50. RG2001*. doi:10.1029/2011RG000369.

Tryner J., L'Orange C., John Mehaffy J., Daniel Miller-Lionberg D., Hofstetter J., Ander Wilson A., Volckens J. Laboratory evaluation of low-cost PurpleAir PM monitors and in-field Correction using co-located portable filter samplers. 2020. *Atmos. Environ.* https://doi.org/10.1016/j.atmosenv.2019.117067.

TROPOMI ATBD of the UV Aerosol Index. July 2022. S5P-KNMI-L2-0008-RP, issue 2.1.0.

Winker M. D., Vaughan M. A., Omar A. L., Hu Y., Powell K. A., Liu Z., Hunt W., Young S.. 2009. *J. Atmos. Ocean. Technol.,* Volume 2. DOI: 10.1175/2009JTECHA1281.1.

Wooster, M., Xu, W., & Nightingale, T. Sentinel-3 SLSTR active fire detection and FRP product: pre-launch algorithm development and performance evaluation using MODIS and ASTER datasets. 2012. *Remote Sens. Environ.*, 120, 236–254. http://dx.doi.org/10.1016/j.rse.2011.09.033.

Wooster M. J., Freeborn P. H., Archibald S., Oppenheimer C., Roberts G. J., Smith T. E. L., Govender N., Burton M., and Palumbo I.. Field determination of biomass burning emission ratios and factors via open-path FTIR spectroscopy and fire radiative power assessment: headfire, backfire and residual smouldering combustion in African savannahs. 2011. *Atmos. Chem. Phys.*, 11, 11591–11615, 2011 doi:10.5194/acp-11-11591-2011.

Wooster, M. J., Zhukov, B., & Oertel, D. Fire radiative energy for quantitative study of biomass burning: derivation from the BIRD experimental satellite and comparison to MODIS fire products. 2003. *Remote Sens. Environ.*, 86, 83–107.

International Journal of Engineering, Sciences and Technologies
ISSN : 3079-2045
https://www.ij-est.org/
Volume 2, issue 1, https://doi.org/10.70961/IKDY7329

7- Figures

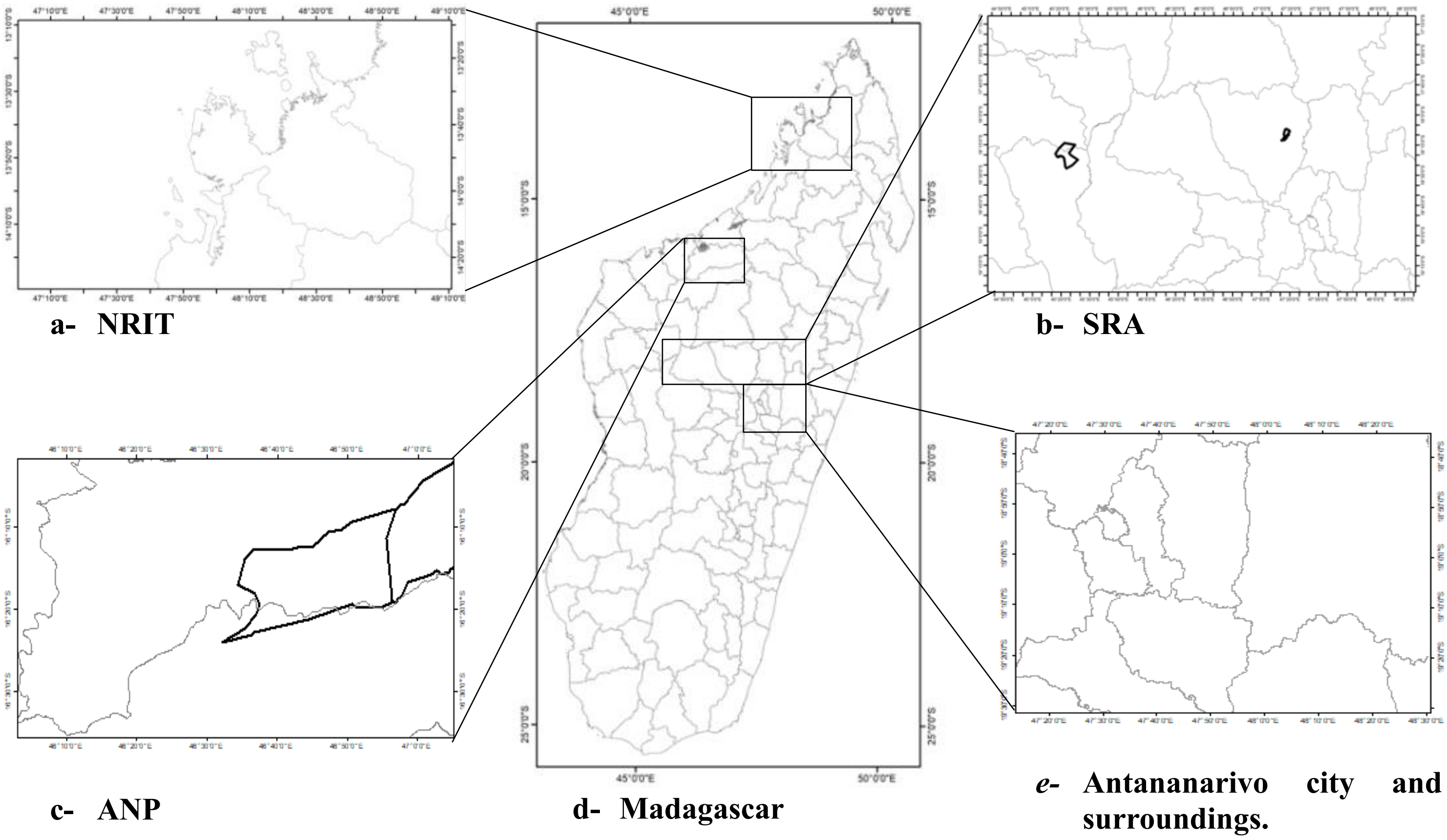

Figure 1: Geographical locations of the study areas. (a) Natural Integral Reserve of Tsaratanana (NRIT). (b) Special Reserve of Ambohitantely (SRA). (c) Ankarafantsika National Parc (ANP). (b) Madagascar. (e) Antananarivo city and surroundings.

International Journal of Engineering, Sciences and Technologies
ISSN : 3079-2045
https://www.ij-est.org/
Volume 2, issue 1, https://doi.org/10.70961/IKDY7329

1- General situation

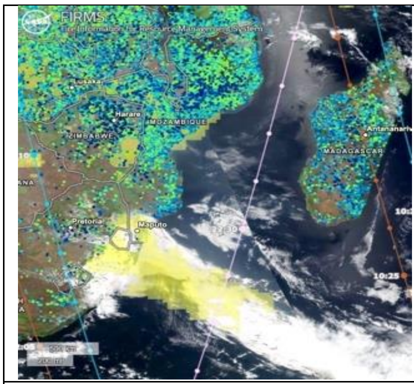	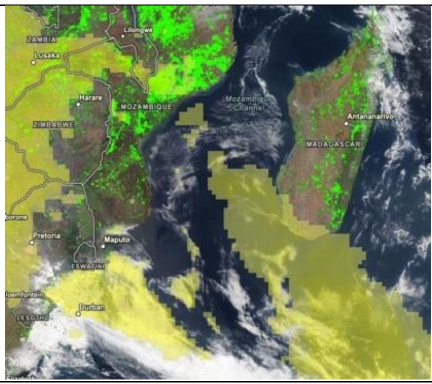	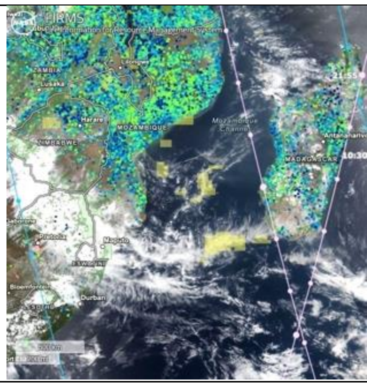
a- 3 October. FRP. UVAI	**b- 7 October. Burnt Areas. UVAI**	**c- 27 October. FRP. UVAI**

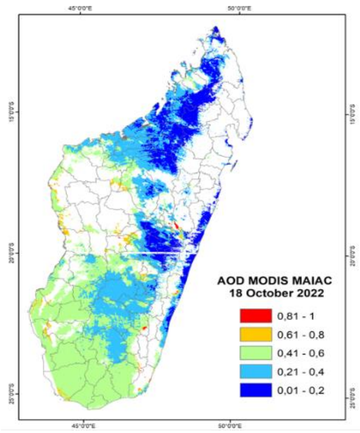

d- 18 October . AOD

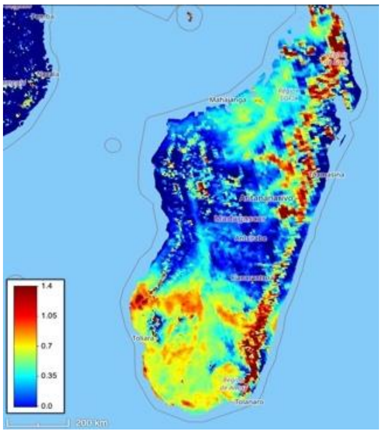

e- 18 October. UVAI

Figures 2: General overview. S-NPP-VIIRS, MODIS, OMPS. Sentinel 5P TROPOMI. October 2022
(Credit FIRMS NASA, Copernicus)

a - 10/03/2022. Fire Pits-FRP– OMPS. UVAI (BrC) yellow area

b – 10/07/2022 Burnt area October 2022 – yellow OMPS UVAI -OC (BrC).

c - 10/27/2022. Yellow: UVAI (BrC)- OMPS – large scale advection ended.
Pollutants dissipated.

d - 10/18/2022-10:40 UTC. MODIS- Deep Blue- AOD MAIAC.
South: AOD up to 0.6 (large-sacle advection from South Africa.
Center: Non absorbing and AOD > 1 near fire clusters.
North-West low AOD.

e - 10/18/2022-10:40 UTC Sentinel 5P TROPOMI UVAI OC (340nm and 380nm).
South- North-Ouest: mostly absorbing aerosols.
Center: Non absorbing. Pits of Absorbing aerosols.
Center West and East: clouds

a

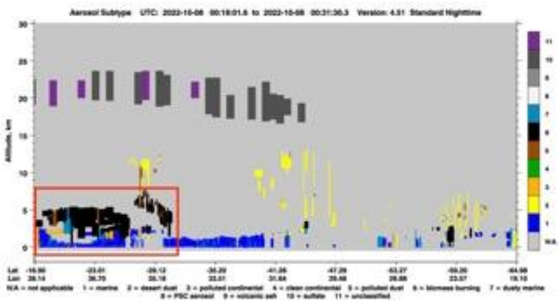

b

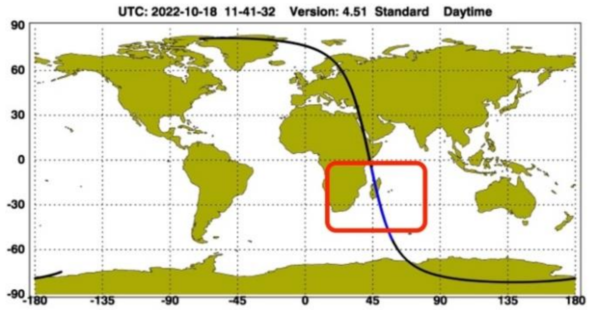

c

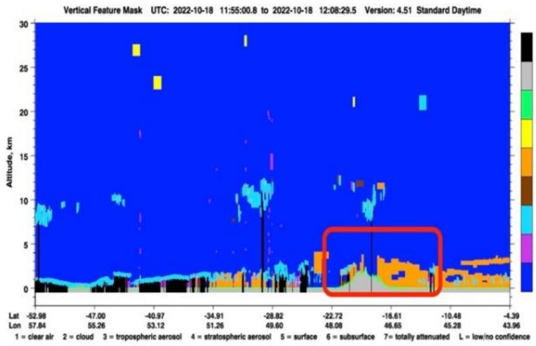

d

Figures 3 : CALIPSO-Aerosol profile. Black Smoke Biomass Burning South-East Africa.

a and b : 07/10/2022 . CALIPSO track and Black Smoke presence.
Biomass burning-related up to 5km ASL initially over South-East of Africa.

c and d : 18/10/2022. CALIPSO track and tropospheric aerosols profile (brown).
Aerosol layers over Madagascar lay below 3km ASL i.e. 1.5 km AGL for Antananarivo and surroundings and Madagascar (and throughout October 2022).

INTERNATIONAL JOURNAL OF ENGINEERING, SCIENCES AND TECHNOLOGIES
ISSN : 3079-2045
International Journal of Engineering, Sciences and Technologies
ISSN : 3079-2045
https://www.ij-est.org/
Volume 2, issue 1, https://doi.org/10.70961/IKDY7329

2- Case studies

Case study 1: Ankarafantsika National Parc (ANP)

Fire ignition on 29 September, max. 10 October & 12 October 2022. Fire temporary extinction on 15 October. Restart on 18 October.

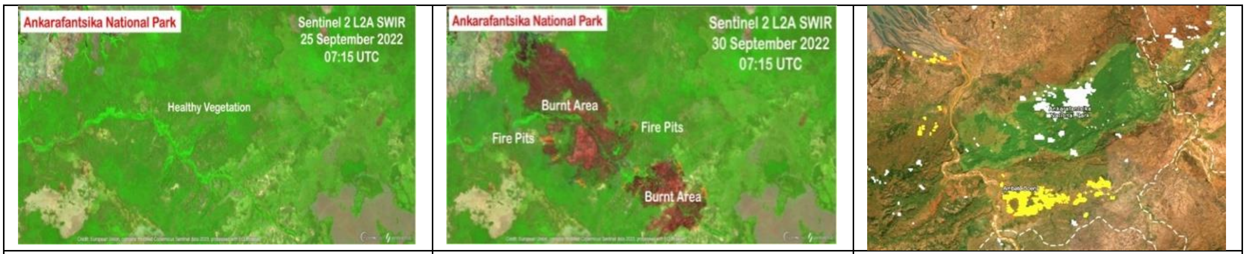

a - 09/25. No fire	b - 09/30. Fires in progress	c - Burnt Areas. April & October 2022

Figures 4: Sentinel 2 L2A – October 2022-SWIR. Ankarafantsika National Parc (ANP) and surroundings (primary humid and dry forests & savannah).

- **a.** Healthy vegetation. No fires.
- **b.** Extended burnt areas (after ignition 2 days before).
- **c.** White area: Total burnt areas October 2022 (forests: primary-secondary & savannahs).

  Yellow area: Total burnt area April 2022 (agriculture waste-rice fields - Boeny)

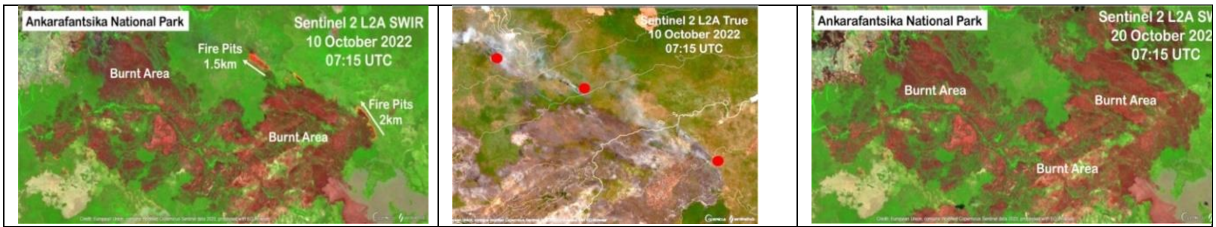

a - 10/10. Fires Pits max intensity	b Zooming . 10/10 Reflectance True Color	c . Final step 10/20 Total burnt area

Figures 5 : Sentinel 2 L2A October 2022 SWIR. (cont'd). ANP. (Credit Copernicus)

- **a.** Larger extended burnt areas with maximum fire intensity (see FRP).
  Fire pits length: 1.5km to 2km. Smaller width (fires on forest edge and savannah)
- **b.** Smokes: primary forest edges (fire front pits-circle red)
- **c.** Fires final step on 20 October. Total burnt areas. Compare to Figure 3a.

International Journal of Engineering, Sciences and Technologies
ISSN : 3079-2045
https://www.ij-est.org/
Volume 2, issue 1, https://doi.org/10.70961/IKDY7329

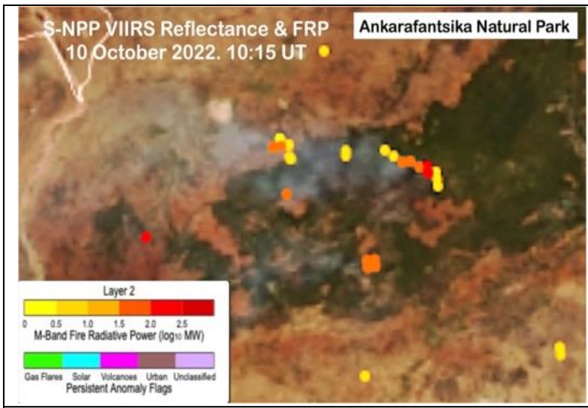

a-10 October - 10:15 UTC
S-NPP VIIRS

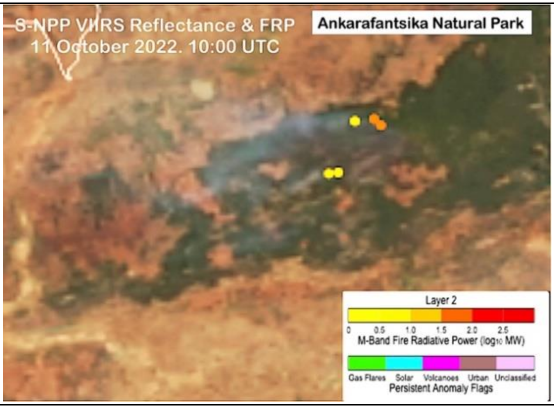

b-11 October - 10:00 UTC
S-NPP VIIRS

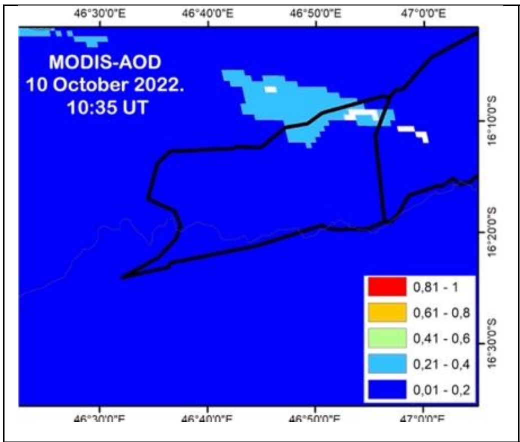

c -10 October -10:35 UTC
MODIS-DB

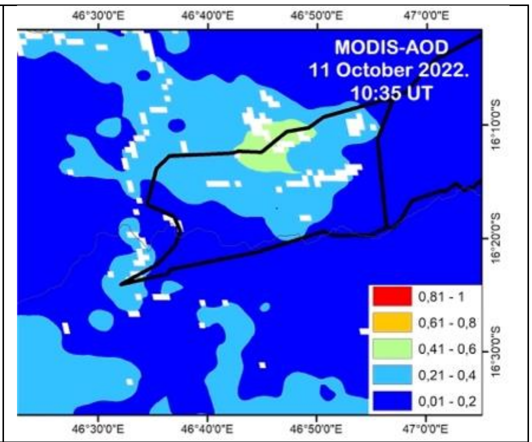

d – 11 October -10:35 UTC
MODIS-DB

Figures 6 : S-NPP VIIRS & MODIS

a -SNPP VIIRS True color (reflectance) & FRP. October 2022. **(**Credit JSTAR NOAA)
FRP-yellow (>=5MW)- Pits
FRP-brown (>=35MW)- Pits
FRP- red (>>100MW) -Pits

b - SNPP VIIRS True color (reflectance) & FRP. October 11

c - MODIS-DB – AOD . Plume expansion to smaller width. AOD= 0.4 in plume

d - MODIS-DB – AOD . Plume expansion to larger area. AOD = 0.4-0.6 in plume center. More smoldering fires.

International Journal of Engineering, Sciences and Technologies
ISSN : 3079-2045
https://www.ij-est.org/
Volume 2, issue 1, https://doi.org/10.70961/IKDY7329

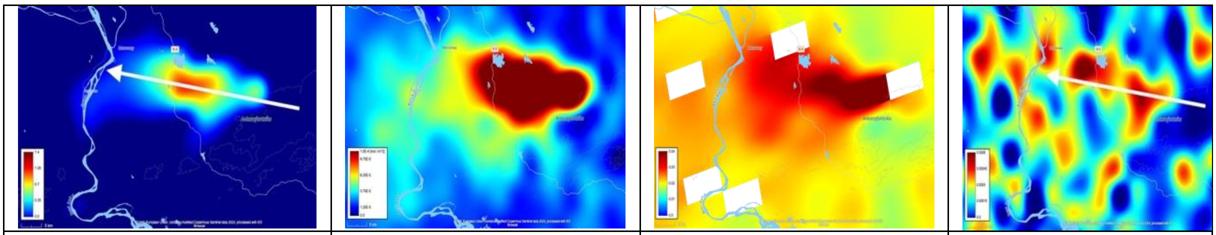

a- 10 October max UVAI = 1.5	**b- NO_2. 10 October max >>10^{-4} mol/m^2**	**c-CO. 10 October max >> 4.10^{-2} mol/m^2**	**d -10 October Blobs. Chaotic**

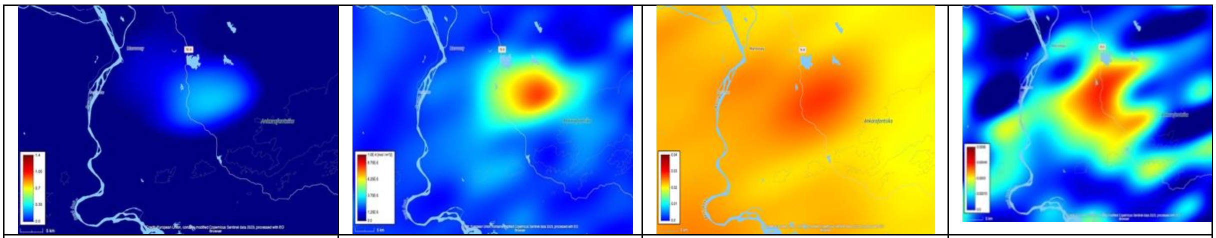

e . 11 October max UVAI = 0.35	**f- 11 October max 6.5 10^{-5} mol/m^2**	**g-11 October max >> 4.10^{-2} mol/m^2**	**h-11 October blobs**

Figure 7 a-b-c-d: Sentinel 5P TROPOMI species column. 10 October 2022 at 09:50 UTC.

a- Sentinel 5P- TROPOMI UVAI (circle -fire). 09:50 UTC.

b- NO_2. Plume expansion “shrinked” - Short-lifetime species.

c- CO . Plume expansion and mixing related to CO longer lifetime.

d- HCHO (arrow : plume expansion). Lower values at fire center. Spatially variable during plume expansion (blobs). Chemically active (e.g. by photodissociation). Source of OH.

Figure 7 e-f-g-h: Sentinel TROPOMI species column. 11 October 2022 at 09:50 UTC

e- Lower absorbing aerosols.

f-g-h lower NO_2-CO-HCHO.

International Journal of Engineering, Sciences and Technologies
ISSN : 3079-2045
https://www.ij-est.org/
Volume 2, issue 1, https://doi.org/10.70961/IKDY7329

Case study 2: Natural Integral Reserve of Tsaratanana (NRIT)

Fire ignition: 25 September 2022. Fire extinction 26 October 2022. 30 days

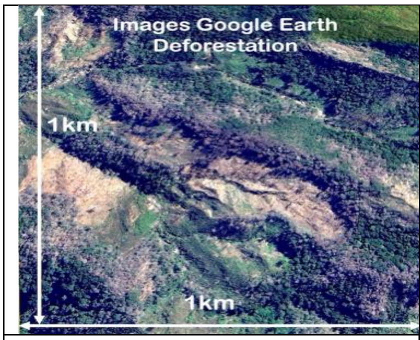

a-Google Earth
Image size 1km²

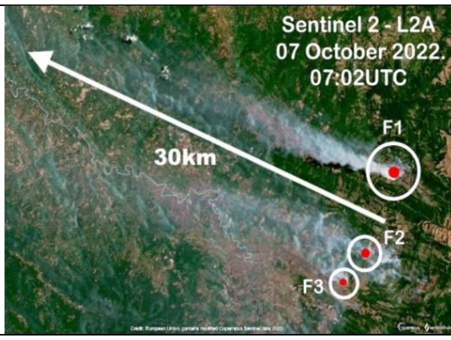

b – 07 October- 07:02 UTC
True color. Fires

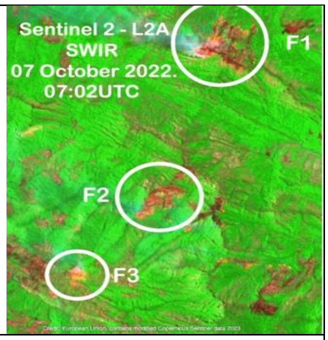

c - 07 October-
07:02UTC. SWIR.

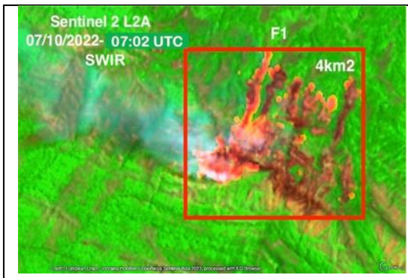

d – 07 October. 07:02 UTC
Fire 1 pits SWIR

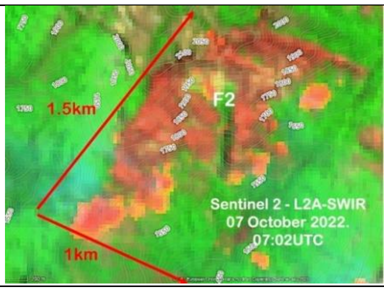

e – 07 October. 07:02 UTC
Fire 2 pits SWIR

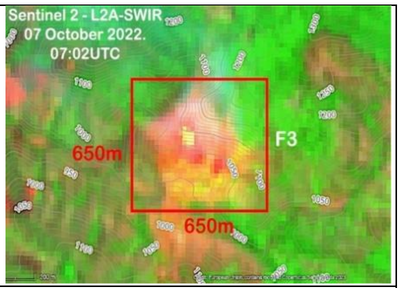

f – 07 October. 07:02 UTC
Fire 3 pits SWIR

Figures 8: Sentinel 2 L2A. SMIR & True Color. 7 October 2022. Large flaming front fire size.

(Credit Copernicus)

a - Google Earth ecosystem with deforestation and clearance by fires.

b – Sentinel 2 L2A True Color. Fire Pits: F1-F2-F3 on 10/07/2022 - 07:02 UTC

c – Sentinel 2 L2A SWIR. Fire Pits F1-F2-F3 on 10/07/2022 - 07:02 UTC

d - Zooming F1 fire pits size: 2km by 2km – flaming + smoldering

e - Zooming F2 fire pits size: 1.5km by 1km – flaming + smoldering

f - Zooming F3 fire pits size: 0.65 km by 0.65 km – flaming + light smoldering

International Journal of Engineering, Sciences and Technologies
ISSN : 3079-2045
https://www.ij-est.org/
Volume 2, issue 1, https://doi.org/10.70961/IKDY7329

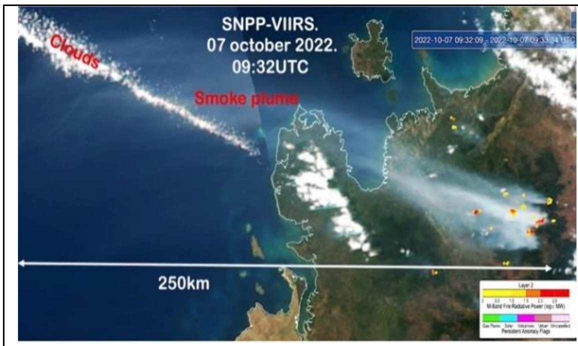	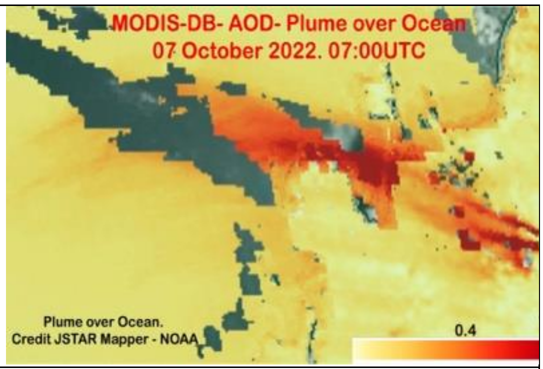
a- Fire pits (FRP) & Reflectance True Color 7 October. 09:32UTC	**b- MODIS -DB AOD 7 October. 0700 UTC**

Figures 9: **S-NPP VIIRS and MODIS- 7 October 2022 (Credit NOAA)**

a - VIIRS True Color observations along with FRP. 09:32 UTC
Fire plumes are visible over 250km distance over ocean downwind.
FRP exhibits >> 100MW value (red points)

b - MODIS-DB AOD 10/07- 0700 UTC. 250km plume of AOD >1.

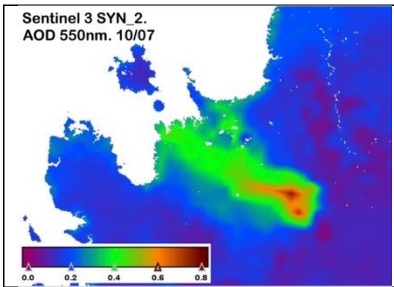	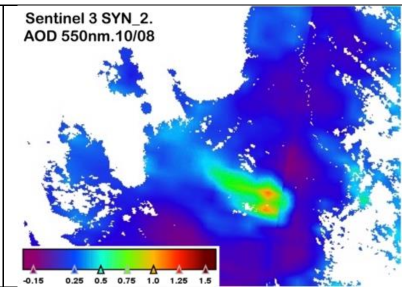	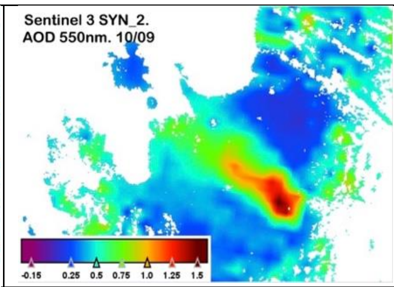
a- 7 October. 06:45 UTC AOD max= 0.8	**b- 8 October. 06:30 UTC AOD max 1.1**	**c- 9 October. 06:30 UTC AOD max= 1.5**

Figures 10: Sentinel 3 SYN_2

a- AOD 550nm. 10/07/2022. 06:45UTC. Maximum 0.8 at fire center (3 pits)
0.4 in the far plume.

b- AOD 550nm. 10/08/2022. 06:45UTC. Maximum 1.1 at fire center and 0.8 elsewhere

d- AOD 550nm. 10/09/2022. 06:30UTC. More fire number and intense (not shown).
Larger surface area of AOD with maximum = 1.5 compared to 10/07.

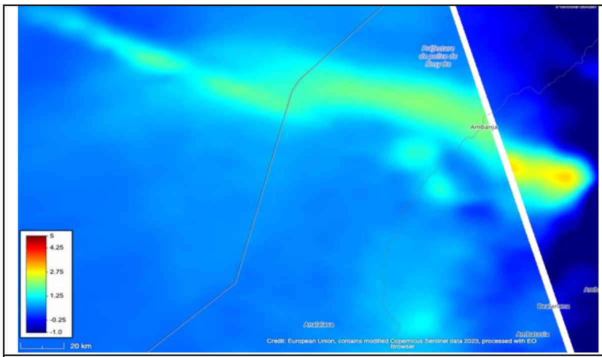	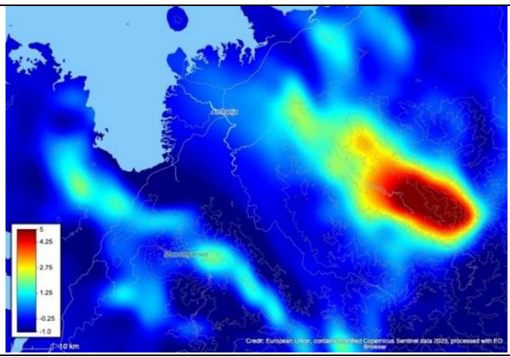
a- UVAI 07 October 09:34UTC (shift error on plotting)	**b -UVAI 09 October 10:12UTC**

3 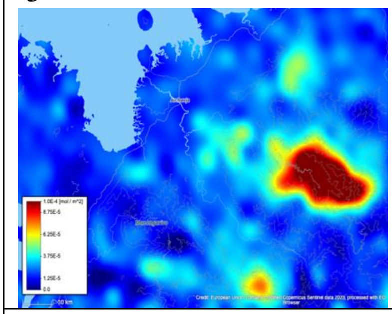	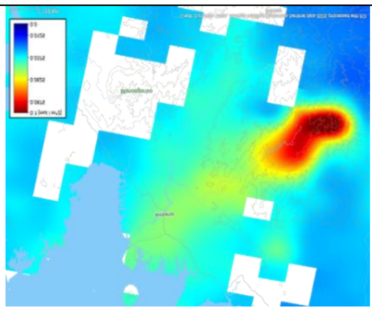	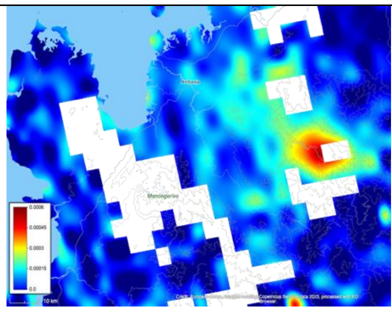
c - NO_2 09 October 10:12 UTC	**d - CO. 09 October 10:12 UTC**	**e – HCHO. 09 October 10:12 UTC**

Figures 11: Sentinel 5P- TROPOMI. (Credit Copernicus)

a- UVAI 10/07-09:34 UTC. Maxima = 3 greater than for ANP forest burning.

b-UVAI 10/09-10:12 UTC. Maxima = 5 largely greater than for ANP forest burning.

c- NO_2 10/09-10:12 UTC. Maxima > to ANP and similar shape

d- CO 10/09-10:12 UTC. Maxima >> to ANP and similar shape

e- HCHO 10/09-10:12 UTC. Shape non chaotic (QA not eligible) for information only.
Possible different reactivity due to different ecosystems and local environment

Case Study 3: Special Reserve of Ambohitantely (SRA)

Primary dense forests and savannah

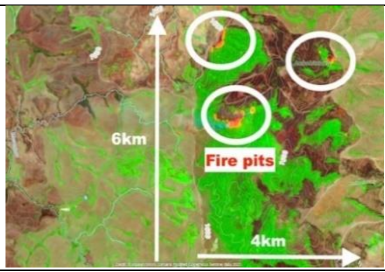

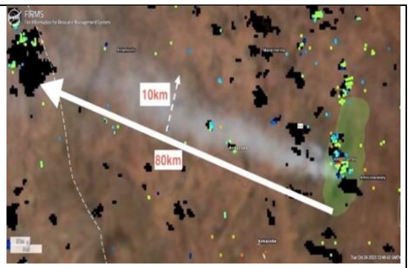

a -Tampoketsa Typical Ecosystem Image size 3km	b – 12 October. 07:05 UTC (no S2 L2A on 11October)	c - 11 October. 10:15 UTC (Image size = 100km)

Figure 12: SENTINEL MSI

a-Google Earth image of Tampoketsa ecosystems.

b- Sentinel 2 L2A SWIR. 12 October 2022. Small fire pits (yellow-red) are detected. Burnt areas by SWIR shown in brown and vegetation in green.

c- SNPP - VIIRS. Surface reflectance True Color.
Black area: total burnt areas for October 2022.
FRP and fire pixels VIIRS-SNPP-NOAA-MODIS AQUA-TERRA- METEOSAT 11 depicted.

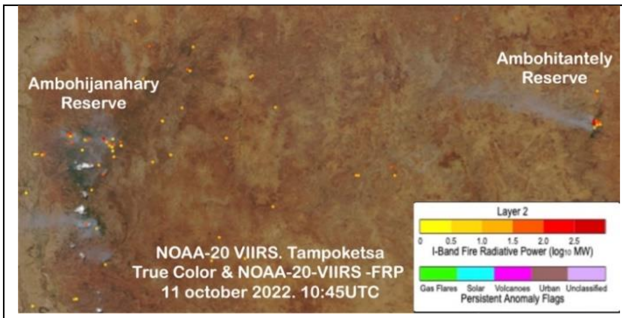

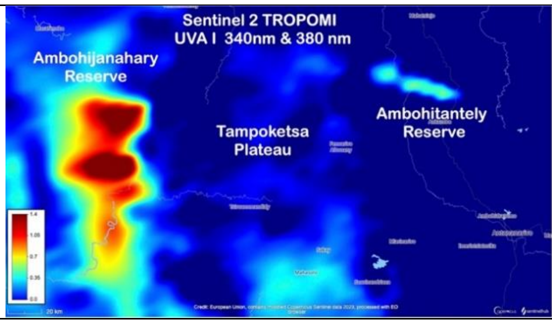

a-Reflectance True Color & FRP Tampoketsa. 10/11/2022 10:45 UTC	b-UVAI. Tampoketsa. 10/11/2022. 10:00 UTC

Figures 13: NOAA 20 & SENTINEL 5P TROPOMI

a- Reflectance NOAA 20- VIIRS- True color. 11 October 2022. 10:45UTC.

b- SENTINEL 5P TROPOMI . UVAI at 10:00 UTC.

International Journal of Engineering, Sciences and Technologies
ISSN : 3079-2045
https://www.ij-est.org/
Volume 2, issue 1, https://doi.org/10.70961/IKDY7329

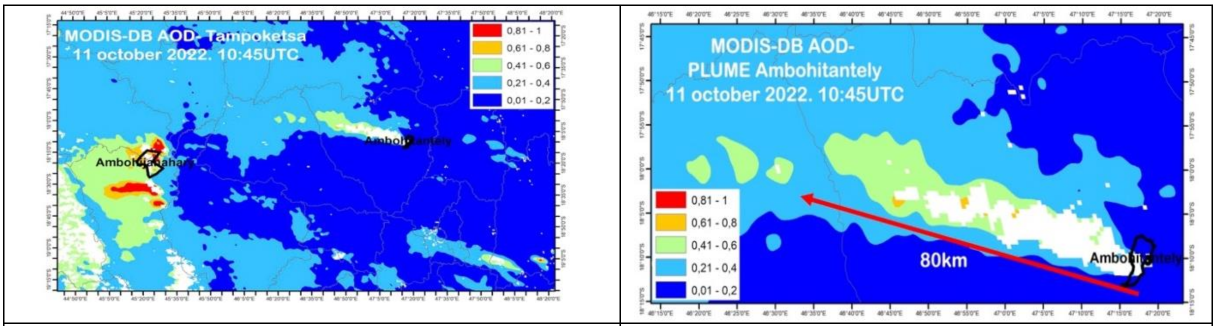

a- MODIS-DB AOD Tampoketsa 11 October -10:45UTC	b- MODIS-DB AOD Local PLUME 11 October. 10:45UTC

Figure 14: MODIS-DB AOD.

a- 11 October 2022 10:45 UTC. Tampoketsa AOD distribution.
Note the well-mixed distribution between 0.2 and 0.4 northern part of Tampoketsa and the low value at the center. Main biogenic fuel herbaceous and localized forests under scattered fires.

b- 11 October 2022 10:45 UTC. Ambohitantely Reserve AOD plume followed by expansion

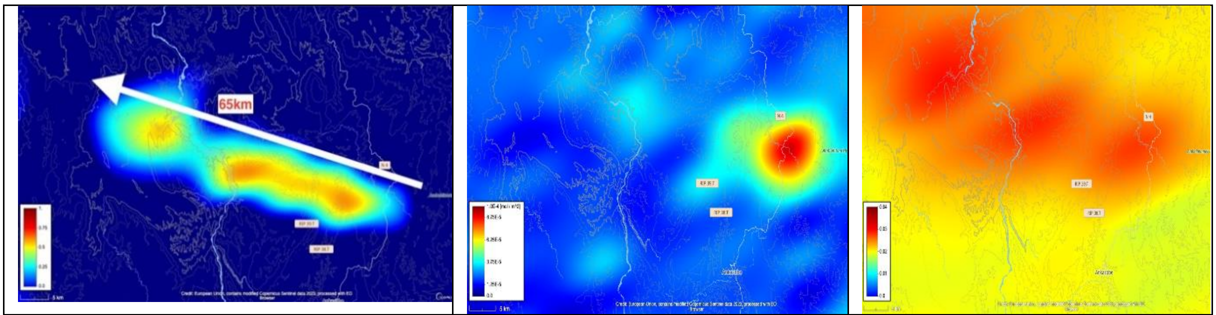

a-UVAI 11 October	b -NO_2 11 October	c - CO 11 Ocober

Figures 15 : SENTINEL 5P TROPOMI

a- UVAI 65 km plume length Sentinel TROPOMI 11 October 2022. 10:00 UTC. UVAI max 0.6. Lower absorbing aerosols inside Ambohitantely plume.

b- Sentinel TROPOMI NO_2 11 October 2022. 10:00UTC. Maximum near centers as usual.

c - Sentinel TROPOMI CO (with stripes) 11 October 2022. 10:56 UTC.

International Journal of Engineering, Sciences and Technologies
ISSN : 3079-2045
https://www.ij-est.org/
Volume 2, issue 1, https://doi.org/10.70961/IKDY7329

Cas 4: Antananarivo city and surroundings.

7 et 27 October 2022

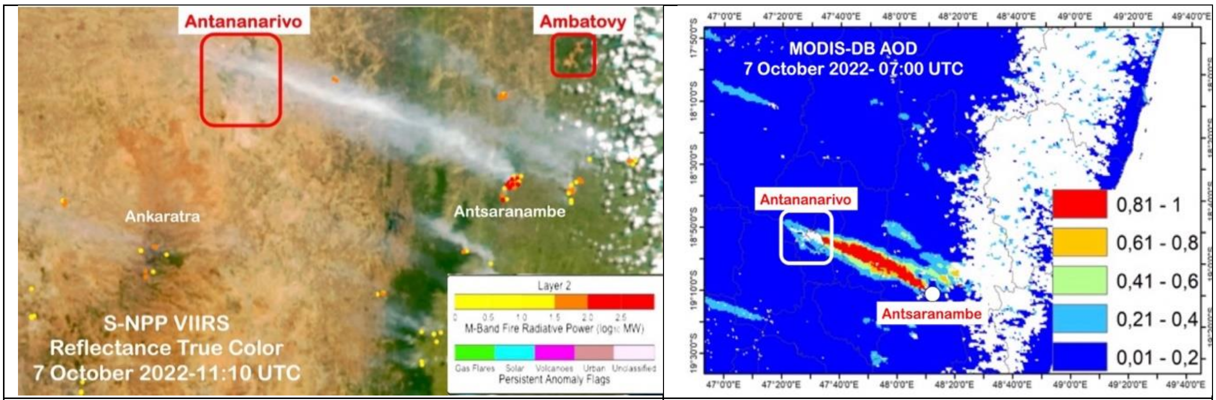

a- S-NPP. VIIRS 7 October. 11:10UTC	b- MODIS -DB AOD 7 October. 07:00UTC

Figures 16: S-NPP- VIIRS- MODIS 7 October 2022

- **a-** Reflectance & FRP at 11:10 UTC. Plumes well developed after 3 hours of MODIS observations
- **b-** MODIS-DB AOD >1. inside principal plume from Antsaranambe at 07:00UTC elsewhere AOD plumes 0.2-0.4 and AOD lower <0.2 background

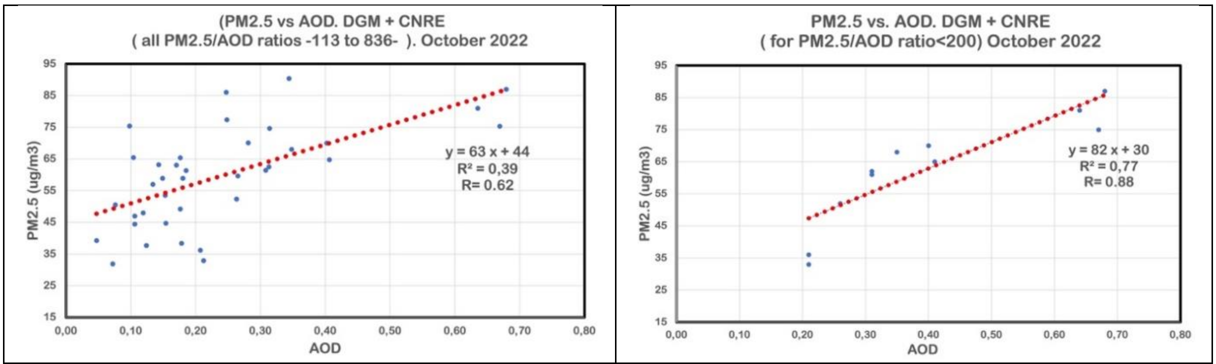

a- $PM_{2.5}$ vs. AOD (all)	b- $PM_{2.5}$ vs. AOD (ratio <200-see text)

Figures 17 : MODIS- Purple air $PM_{2.5}$. Octobre 2022

a- $PM_{2.5}$ vs AOD for all $PM_{2.5}$/AOD

b- $PM_{2.5}$ vs AOD for $PM_{2.5}$/AOD < 200- see text.

International Journal of Engineering, Sciences and Technologies
ISSN : 3079-2045
https://www.ij-est.org/
Volume 2, issue 1, https://doi.org/10.70961/IKDY7329

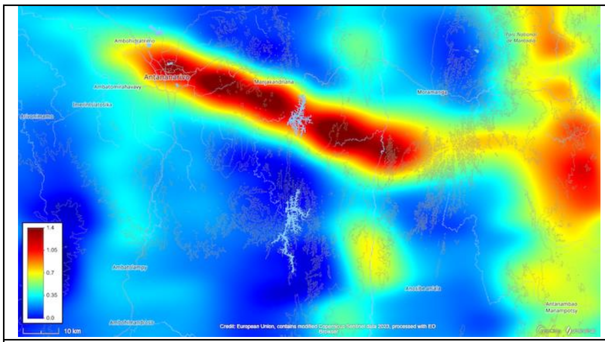

a- UVAI 10:50 UTC

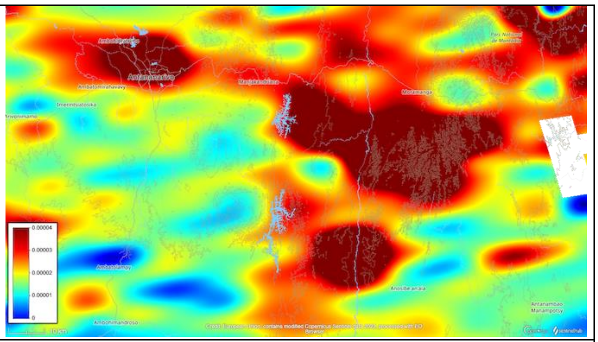

b- NO_2 10:50UTC

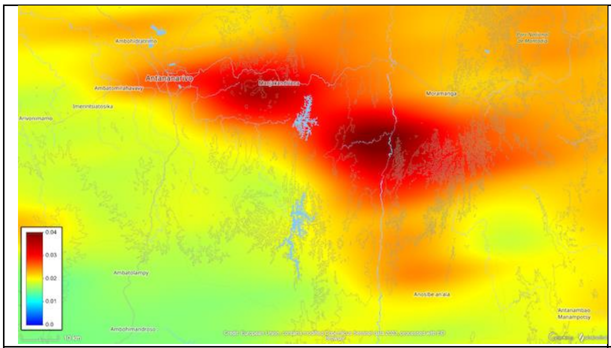

c- CO 10:50UTC

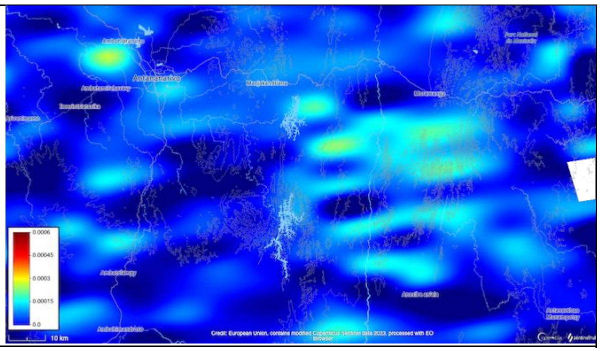

d- HCHO 10:50 UTC

Figures 18 : Sentinel 5P TROPOMI 7 October 2022

a- BrC plume transported from Antsaranambe (UVAI max =1.4) superimposed on local ground transport emissions in the city of Antananarivo.

b- Despite its short lifetime, plume of high NO_2 is transported downwind to the city superimposed to the city émissions**.**

c- A dispersed longer lifetime CO plume, superimposed on city emissions.

d- Blobs of HCHO plume from Antsaranambe to Antananarivo related to its reactivity. HCHO is shown to be ea fire-product herein emitted in the fire.

International Journal of Engineering, Sciences and Technologies
ISSN : 3079-2045
https://www.ij-est.org/
Volume 2, issue 1, https://doi.org/10.70961/IKDY7329

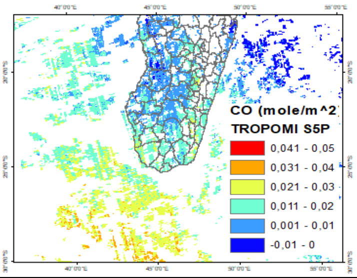

a-Diff. between 16 and 30 Oct. 2022

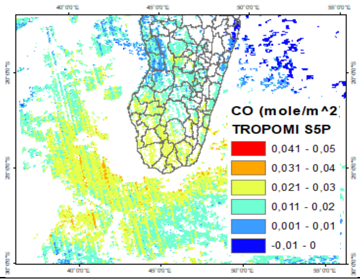

b- Diff. between 18 and 30 Oct. 2022

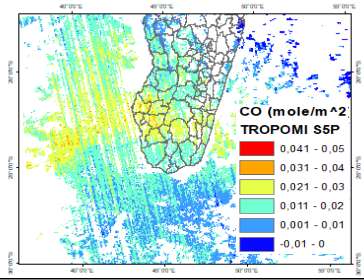

c- Diff. between 19 and 30 Oct. 2022

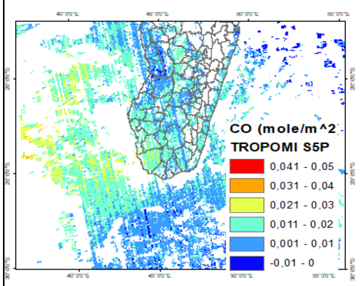

d- Diff. between 20 and 30 Oct. 2022

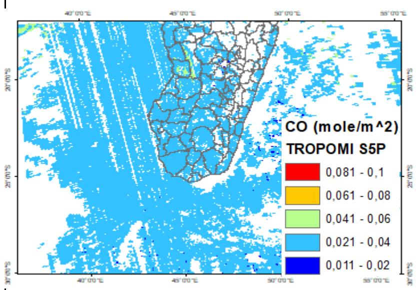

e-30 Octobre 2022. Reference day.

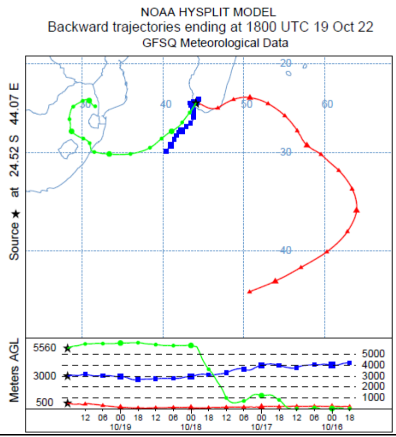

f-Backward trajectories

Figure 19 : “Difference between pollution days (16th to 20th October) and reference day (30th October) of CO concentration observed by TROPOMI S5P.

a and b - Smoke river advected into the Indian Ocean.

c and d- Passage of a front marked by the incursion of CO into the south of Madagascar.

e- Reference day 30/10. More diffused CO concentration. Disappearance of smoke river.

f- Backward trajectories simulated by HYSPLIIT for 96 hours ending on 2022/10/19 at 18 UTC. Ascendance and transport to Madagascar from 2022/17/10.